RESEARCH ARTICLE

CrossMark

Roles of hydrophobic and hydrophilic fractions of dissolved organic matter in sorption of ketoprofen to biochars

Lin Wu[1] · Ningwei Yang[1] · Binghua Li[2] · Erping Bi[1]

Abstract

Hydrophobic acid (HoA) and hydrophilic neutral (HiN) are two major fractions of dissolved organic matter (DOM). Their role in the sorption of ketoprofen (KTP) to wheat straw-derived biochars pyrolyzed at 300 °C (WS300) and 700 °C (WS700) was investigated to further probe the mechanisms responsible. WS700 has much higher pore volume and specific surface area (SSA) than WS300. Loading of HoA and HiN resulted in surface coverage of biochars. HoA with larger molecular size led to more pore blockage of biochars than HiN. Higher HoA binding affinity also caused a stronger competition with KTP on biochars. These factors reduced the accessibility of sorption sites for KTP, and significantly inhibited KTP sorption to biochar of lower SSA (i.e., WS300) by HoA. Water solubility (S_w) of KTP was slightly enhanced (3%) in the presence of HoA. In contrast, the presence of HiN reduced (22%) S_w of KTP. The decreased S_w of KTP by HiN exerted a more dominant influence than its competitive and loading effects, thus led to apparent enhanced sorption of KTP, especially to biochar of higher SSA (i.e., WS700). The results demonstrated the diverse effects of HoA and HiN on KTP sorption, which is helpful in understanding pharmaceutical-DOM-biochar interactions and environmental behaviors of pharmaceuticals.

Keywords Ketoprofen · Biochar · Sorption · Solubility · Dissolved organic matter (DOM) · DOM fractions

Abbreviations

KTP	Ketoprofen
WS300	Wheat straw-derived biochar at 300 °C
WS700	Wheat straw-derived biochar at 700 °C
DOM	Dissolved organic matter
DOC	Dissolved organic carbon

Highlights

- Loading of HoA and HiN resulted in surface coverage and pore blockage of biochars.
- HoA has larger molecular size and higher binding affinity to biochars than HiN.
- Competition of HoA significantly inhibited KTP sorption to biochar of lower SSA.
- HiN could enhance KTP sorption to biochars by reducing solubility of KTP.
- KTP sorption enhancement by coexisting HiN is pronounced on biochar of higher SSA.

Responsible editor: Philippe Garrigues

✉ Erping Bi
  bi@cugb.edu.cn

  Lin Wu
  wulinline@163.com

  Ningwei Yang
  ningweiv@126.com

  Binghua Li
  libinghua75@163.com

[1] School of Water Resources and Environment, Beijing Key Laboratory of Water Resources and Environmental Engineering, and MOE Key Laboratory of Groundwater Circulation and Environmental Evolution, China University of Geosciences (Beijing), Beijing 100083, China

[2] Beijing Water Science and Technology Institute, Beijing 100048, China

HoA   Hydrophobic acid
HiN   Hydrophilic neutral
HPLC   High performance liquid chromatography
SSA   Specific surface area
SEM   Scanning electron microscope

Introduction

In recent years, anti-inflammatory pharmaceuticals are emerging organic pollutants, which have gained increasing public and scientific attention due to their wide presence in the environment and potential risk to human health (Fick et al. 2009; Stuart et al. 2012; Yang et al. 2017). Sorption is an important process that controls the transport and environmental risks of these organic pollutants (Doucette 2003; Metzelder et al. 2018). Recent studies have indicated that biochar, which is produced by heating biomass under oxygen-limited conditions and widely used as a soil amendment, plays a significant role in sorption of organic pollutants (Jin et al. 2016; Kumari et al. 2014; Zhang et al. 2017). Pyrolysis temperature is a key factor that influences the nature of biochar and its sorption properties for organic pollutants (Xiao et al. 2014). Typically, biochar produced at relatively low temperatures is not fully carbonized and sorption of neutral organic pollutants to it is controlled by absorption (i.e., partition) (Chen et al. 2008; Chen et al. 2012a). Biochar produced at high temperatures is well carbonized and adsorption interactions (e.g., π-π interactions and H-bond) are the main sorption mechanisms for organic pollutants (Kah et al. 2017; Keiluweit and Kleber 2009).

Dissolved organic matter (DOM) is widely present in the environment. Sorption of pharmaceuticals by biochar applied to soil might be greatly affected by soil DOM (Oh et al. 2016; Pan et al. 2013). Previous studies have shown that DOM can decrease or enhance sorption of organic pollutants to carbonaceous materials on account of its varied interactions with them, including competition for sorption sites (Shimabuku et al. 2014) and binding with organic compounds (Bedard et al. 2014). As DOM is a diverse and complex mixture of compounds, it can be fractionated based on its hydrophobic characteristics (Straathof and Comans 2015). The proportion of hydrophobic and hydrophilic fractions varies in different DOM samples, which is mainly caused by the difference in origin, maturity level, storage time, and concentration of DOM (Chefetz et al. 1998). It was reported that hydrophobic acid (HoA) and hydrophilic neutral (HiN) are two major fractions of DOM (Maoz and Chefetz 2010; Xue et al. 2009; Yang and Bi 2017), which might control the binding of organic pollutants to DOM. For example, HoA plays an important role in governing the sorption of triazine herbicides by DOM (Ilani et al. 2005).

The fractionation scheme of DOM based on its hydrophobic characteristics has provided valuable mechanistic information on the interaction between DOM and organic pollutants. For instance, binding of pyrene to hydrophobic neutral and HoA fractions is controlled by nonspecific interactions and specific π-π interactions, and the higher binding of hydrophobic neutral fraction is mainly because of its greater hydrophobicity, aromaticity, and large molecular size (Mei et al. 2016; Polubesova et al. 2007). Among the hydrophilic fractions, the hydrophilic acid fraction exhibits the highest sorption affinity for carbamazepine, probably due to its bipolar characteristics (Maoz and Chefetz 2010). However, research on the roles of various hydrophobic and hydrophilic fractions of DOM extracted from soil in sorption of organic pollutants by different sorbent is quite limited (Chen et al. 2011), and urgently needed to clarify the overall binding properties.

Ketoprofen (KTP) is a nonsteroidal anti-inflammatory and analgesic drug. It is introduced primarily after medication via urinal or fecal excretion into sewage treatment plants, where it is not eliminated efficiently due to its lipophilic and biologically persistent characteristics (Xu et al. 2009). KTP was frequently detected in wastewater effluents and surface waters at levels ranging from nanogram per liter up to microgram per liter and has raised potential concerns (such as the enhanced toxicity of chemical mixtures and development of antibiotic-resistant bacteria) in recent years (Tixier et al. 2003). In addition to the occurrence in aquatic environments, KTP can also be introduced into agricultural soil via treated wastewater irrigation. Biochar applied to soil thus has the potential to sequester KTP due to its high sorption capacity. Previous research has shown that there is a positive relationship between KTP sorption and the organic carbon content of the soils and sediments (József et al. 2012; Xu et al. 2009). In addition, dissociation of KTP would decrease its sorption due to the low hydrophobicity of anionic species (Wu et al. 2017). However, influence of hydrophobic and hydrophilic fractions of DOM on KTP sorption to biochars has not been studied, which is important in gaining a better understanding of KTP-DOM-biochar interactions and environmental behaviors of KTP.

The purpose of this study was to identify the roles of hydrophobic and hydrophilic fractions of DOM in sorption of KTP to biochars. HoA and HiN were selected as representative hydrophobic and hydrophilic fractions of DOM, respectively. DOM fractions (i.e., HoA and HiN) and biochars with different degrees of carbonization were prepared and characterized. Batch experiments on KTP, HoA, and HiN sorption to biochars in both single solute and bisolute systems, and dialysis bag experiments of KTP sorption to HoA and HiN were carried out. Dissolved organic carbon from biochars and solubility of KTP in different solutions were also examined. Sorption data was fitted by suitable models and discussed.

Materials and methods

Chemicals

KTP (> 98.0%) was purchased from Tokyo Chemical Industry (Japan). Selected physicochemical properties of KTP are presented in Table 1. Stock solution was prepared by dissolving KTP in methanol from Fisher Chemical Company (Fair Lawn, NJ). The stock solution was diluted with ultrapure water to get the appropriate KTP standard solution for the preparation of standard samples. The solution remained clear after dilution. Acetic acid and NaCl were purchased from Beijing Chemical Works (Beijing, China).

DOM fractionation and characterization

DOM was extracted from natural humus soil collected from Yimeng mountain, China, as a representative natural DOM. The soil was sieved (2 mm) and mixed with deionized water at a ratio of 1 g:10 mL, then the mixture was shaken (175 rpm, 25 ± 1 °C) for 24 h. The suspension was then centrifuged (3000 rpm, 30 min), and the supernatant was filtered through 0.45 μm filters (Millipore, Bedford, MA, USA) and used as DOM solution. HoA and HiN were isolated from the natural humus soil-derived DOM using a published method (Engel and Chefetz 2015; Leenheer 1981). In brief, the DOM solution was acidified to pH 2.0 with 6.0 M HCl and loaded onto a glass column containing XAD-8 resin (Sigma, USA). HoA was displaced from the resin with 0.1 M NaOH. The remaining unsorbed hydrophilic fractions were loaded onto a cation exchanger Amberlyst-15 (Shanghai Aladdin Reagent Co. Ltd., China) and an anion exchanger Amberlyst A-21 (Shanghai Aladdin Reagent Co. Ltd., China) in sequence. HiN was eluted while the other fractions were retained on the resin. The flow rate was less than 10 pore volumes per hour through the glass column. For purification, HoA and HiN were then dialyzed (100 Da, dialysis bags, Union Carbide Corporation, USA) against deionized water for 48 h (change water every 4 h) to remove salts and impurities (Haham et al. 2012).

The concentration of dissolved organic carbon (DOC) in HoA and HiN was determined using a total organic carbon (TOC) analyzer (TOC-3210, Shimadzu, Japan). HoA and HiN were stored at 4 °C and diluted to the appropriate concentrations for further experiments. The freeze-dried HoA and HiN were analyzed for C, H, N, and O contents with a Thermo Scientific FLASH 2000 CHNS/O Elemental Analyzer. The
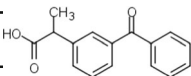
total acidity of HoA and HiN was determined using a titration procedure (Christensen et al. 1998). Ultraviolet absorption of HoA and HiN solution at 465 (E_4) and 665 (E_6) nm was measured using a Shimadzu UV-1800 spectrophotometer. The ratios of the measured absorption values (E_4/E_6 ratios) were calculated to evaluate the aromaticity, molecular weight, and polarity of the samples (Peuravuori and Pihlaja 1997). The hydrodynamic diameters of HoA and HiN were measured by a dynamic light scattering (DLS) method using a ZetaPALS instrument (Brookhaven Instrument Co., USA). Briefly, HoA or HiN solution (30 mg L^{-1}) was poured into a cuvette until the cuvette was filled to the brim. The instrument was operated at 25 ± 1 °C with measuring angle of 90° to the incident beam. Atomic force microscopy (AFM) was used to investigate the conformation of HoA and HiN. Briefly, the freshly cleaved muscovite surface was dipped into HoA and HiN solution (30 mg L^{-1}) to allow sorption of HoA and HiN molecules. The muscovite samples were then placed into deionized water to remove weakly sorbed particles, followed by air drying. The samples were then analyzed using a tapping mode AFM (Dimension Icon, Bruker Co., USA). The scanning speed was maintained at 1.00 Hz. The charge properties of HoA and HiN were determined by zeta potential measurements, which were conducted at pH 3.0, 4.0, 5.0, 6.0 7.0, 8.0, and 9.0 (with concentration of 30 mg L^{-1}) using a Nano-Z Zetasizer (Malvern Instruments Ltd.).

Biochar preparation and characterization

Two biochars were produced from wheat straw at 300 and 700 °C (referred to as WS300 and WS700, respectively) as described in a previous study (Wu et al. 2017). They were chosen as sorbents representing different degrees of carbonization. In brief, wheat straw was placed in a ceramic pot, covered with a fitting lid, and torrefied (at 300 °C) or pyrolyzed (at 700 °C) in a muffle furnace under oxygen-limited conditions for 6 h to prevent calcination of the biomass in the presence of oxygen. For demineralization, the charred residues were treated with 1.0 M HCl for 24 h. The acid was then removed by rinsing the biochars with deionized water until the rinse water reached a pH of 7.0. The biochars were then oven-dried overnight at 80 °C, passed through a 0.38 mm mesh, and stored in foil covered bottle at room temperature (25 ± 1 °C) for subsequent experiments.

The specific surface area (SSA) of biochars was measured by N_2 gas adsorption-desorption at the liquid N_2 temperature using a Micromeritics ASAP 2020 M + C (USA). The

Table 1 Selected physicochemical properties of KTP

Compound	CAS number	Structure	Formula	Molecular weight	pK_a[a]	Log K_{OW}[a]
KTP	22071–15-4		$C_{16}H_{14}O_3$	254.29	4.45	3.12

[a] From SRC Physprop Database

multipoint Brunauer-Emmett-Teller (BET) analysis of the adsorption data points was employed to calculate the SSA. The total pore volume (V_{pore}) was determined from a single-N_2 adsorption point at a relative pressure of 0.95. Elemental (C, H, N) analyses were conducted using an Elementar vario EL (Germany). A scanning electron microscope (SEM, S-4800, Hitachi, Japan) was used to determine the inner structure and morphology of biochars. The elemental composition, SSA, V_{pore}, and SEM images of biochars loaded with HoA and HiN were also obtained. In brief, the HoA and HiN solution (30 mg L^{-1}) was decanted into 20 mL brown glass vials with pre-weighed biochars. Initial solution pH was adjusted to 5.0 using 1.0 M HCl and NaOH. Samples were pre-equilibrated with solid-to-water ratios similar to the sorption experiments. After that, the suspensions were centrifuged at 3000 rpm for 15 min. The residues were rinsed with deionized water and then freeze-dried for measurement.

Sorption experiments

Both batch and dialysis bag sorption experiments were conducted to determine the sorption coefficients according to the different sorbate-sorbent interactions. Sorption of KTP, HoA, and HiN to biochars was conducted by a batch equilibrium method. The 20 mL of sorbate solution (0.01 M NaCl as background electrolyte in ultrapure water) was added into 20-mL brown glass vials after containing biochars (0.02 g of WS300 or 0.003 g of WS700). For KTP isothermal experiments, initial concentrations of KTP were 2, 8, 15, 25, 35, and 45 mg L^{-1} with addition of 0 or 30 mg L^{-1} HoA or HiN (Table 2). For the sorption experiments of HoA and HiN to biochars, initial concentrations of HoA or HiN were 5, 15, and 30 mg L^{-1} with addition of 0 or 30 mg L^{-1} KTP. For sorption experiments of KTP, HoA, and HiN to biochars, initial solution pH was adjusted to 5.0 using 1.0 M HCl and NaOH. The solution pH was also monitored at the end of the experiments and no significant change (within 0.5) was observed. The sample vials were placed on a reciprocal shaker in the dark

at 175 rpm and 25 ± 1 °C for 7 days to reach the apparent equilibrium. After centrifugation (3000 rpm for 15 min for WS300 and WS700, and 12,000 rpm for 10 min for WS300 in succession), the supernatants were taken for further analysis. For samples containing HoA or HiN, the supernatants were filtered through 0.45-μm filters (Millipore, Bedford, MA, USA) before measuring. No obvious solute loss (less than 5%) by the filters was detected.

Sorption coefficients of KTP to HoA and HiN were determined through dialysis bag sorption experiments (Maoz and Chefetz 2010). Dialysis bags (100 Da, Union Carbide Corporation, USA) were boiled in distilled water for 10 min, and washed sequentially with ethanol and distilled water before use. The 10 mL of 30 mg L^{-1} HoA or HiN solution (0.01 M NaCl as background electrolyte) was placed in the dialysis bags. The dialysis bags containing HoA or HiN were placed in 40-mL brown glass vials containing 20 mL of 30 mg L^{-1} KTP solution (0.01 M NaCl as background electrolyte). Initial solution pHs were adjusted to 3.0, 5.0, 7.0, and 9.0 by 1.0 M HCl and NaOH. The vials were placed on a reciprocal shaker in the dark at 175 rpm and 25 ± 1 °C for 7 days. The amount of KTP sorbed to HoA and HiN was determined as the KTP concentrations inside the dialysis bags minus the concentration outside the dialysis bags. KTP sorption to the dialysis bags was negligible (< 1%).

The final methanol volume in fractions from KTP stock solution was kept at < 0.1% (v/v) to avoid co-solvent effects. All experiments were run in duplicate. Blank samples without biochar were regularly run to account for the minor solute loss (such as degradation and sorption to the glass walls) (< 3%). KTP concentration was determined using a high performance liquid chromatography (HPLC) with a 4.6×150 mm reverse phase XDB-C18 column and the UV detector set to 257 nm (HPLC, Shimadzu Corp, LC-20AT, Japan). The mobile phase was methanol-water (70:30, v:v) adjusted to pH 3.0 using acetic acid. The flow rate was 1.0 mL min^{-1}.

Dissolved organic carbon from biochars

The possible dissolution of DOC from WS300 and WS700 at different pHs ranging from 3.1 to 11.6 was measured to assess its effect on KTP sorption. To this end, biochars were mixed with background solution without KTP on a reciprocal shaker in the dark at 175 rpm and 25 ± 1 °C for 7 days. The solid-to-water ratios were identical to those used in sorption experiments. Then, the vials were centrifuged as described above, followed by filtering the supernatants through 0.45-μm microfiber filters (Millipore, Bedford, MA, USA). The DOC concentrations in the supernatants were measured by a TOC analyzer (TOC-3210, Shimadzu, Japan). No obvious DOC loss (< 5%) by the filters was detected.

Table 2 Conditions of batch sorption experiments of KTP, HoA, and HiN to WS300 and WS700 at pH 5.0

Primary (+secondary) sorbate	$C_{i, pri}$[a] (mg L^{-1})	$C_{i, sec}$[b] (mg L^{-1})
KTP	2, 8, 15, 25, 35, 45	0
KTP (+HoA)	2, 8, 15, 25, 35, 45	30
KTP (+HiN)	2, 8, 15, 25, 35, 45	30
HoA	5, 15, 30	0
HoA (+KTP)	5, 15, 30	30
HiN	5, 15, 30	0
HiN (+KTP)	5, 15, 30	30

[a] Initial primary sorbate concentration

[b] Initial secondary sorbate concentration

Solubility tests

Solubility (S_w, mg L^{-1}) of KTP was examined in different solutions under experimental conditions (pH 5.0, 0.01 M NaCl as background electrolyte). An excess of solid KTP was added to solutions with and without HoA or HiN (30 mg L^{-1}), then the vials were shaken (175 rpm, 25 ± 1 °C) for 24 h, centrifuged (3000 rpm for 15 min), and analyzed. Duplicates were measured for all the samples.

Data analysis

Sorption coefficients (K_d, L kg^{-1}) were calculated as:

$$K_d = C_s/C_e \tag{1}$$

where C_s(mg g^{-1}) is the amount of sorbate sorbed per unit mass of sorbent and C_e(mg L^{-1}) is the equilibrium aqueous concentration of sorbate.

Sorption isotherms were fitted with the Freundlich model (Eq. 2), Langmuir model (Eq. 3), and the Dubinin-Astakhov model (Eq. 4):

$$C_s = K_F C_e{}^n \tag{2}$$

$$C_s = Q_m K_L C_e/(1 + K_L C_e) \tag{3}$$

$$\log C_s = \log Q_m - ((RT \ln(S_w/C_e))/E)^b \tag{4}$$

where K_F(mg$^{(1-n)}$L^{n}g^{-1}) is the Freundlich affinity coefficient, n is the Freundlich parameter reflecting the nonlinearity of sorption (nonlinearity increases as n deviates from 1.0),

Q_m(mg g^{-1}) is the maximum sorption capacity, K_L(L mg^{-1}) is the affinity constant, R [8.314×10^{-3} kJ mol^{-1} K^{-1}] is the universal gas constant, T (K) is the absolute temperature, E (kJ mol^{-1}) is the correlating divisor (commonly used to evaluate an average adsorption affinity), and b is a fitting parameter.

Results and discussion

Characterization of DOM fractions and biochars

Elemental analysis demonstrated a greater N content in HiN than that in HoA (Table 3). Higher H/C ratio was observed for HiN than that for HoA (1.7 versus 1.2). In addition, HiN exhibited a lower C/N ratio (10.0 versus 27.7 in HoA). The atomic ratio results indicated that HiN may be rich in peptide-containing compounds like proteinaceous materials with distinct aliphatic nature (Leenheer 1981; Polubesova et al. 2007). The total acidity of HoA was higher than that of HiN (Table 3), which corresponded to its inherent acidic characteristics and indicated appropriate fractionation procedures.

The ultraviolet absorption measurement results showed that the E_4/E_6 ratio of HoA was higher than that of HiN (Table 3), suggesting that HoA had a higher molecular weight, more complicated molecular structure (polyphenol-humic structure), and higher degree of aromaticity (Chefetz et al. 1998; Engel and Chefetz 2015). It can also be seen from the DLS measurement results (Fig. 1a) that the peaks of particle size distribution of HiN and HoA appeared at 117 and 195 nm, respectively. This indicated a generally increasing molecular size from HiN to HoA.

Table 3 Properties of DOM fractions and biochars with and without loaded HoA and HiN

| DOM fraction	Properties of DOM fractions[a]					
	C (%)	H (%)	N (%)	O (%)	Total acidity (mmol g^{-1})	E_4/E_6
HoA	39.86	3.83	1.68	38.63	13.52	18.59
HiN	39.07	5.54	4.56	33.65	7.06	4.43
Biochar[b]	Properties of Biochars					
	C (%)	H (%)	N (%)	O[c] (%)	SSA (m^2 g^{-1})	V_{pore} (cm^3 g^{-1})
WS300	64.88[d]	4.10[d]	0.70[d]	30.32	6[d]	0.008
WS300HoA	63.58	3.71	1.74	30.97	5	0.003
WS300HiN	63.96	4.00	1.51	30.53	5	0.005
WS700	67.82[d]	2.13[d]	0.77[d]	29.28	605[d]	0.421
WS700HoA	62.54	2.62	0.88	33.95	501	0.186
WS700HiN	62.58	3.19	0.83	33.40	454	0.295

[a] From (Yang and Bi 2017)

[b] Biochars with loaded HoA and HiN were abbreviated as WS300HoA/WS700HoA and WS300HiN/WS700HiN, respectively

[c] Determined by mass balance on ash-free basis

[d] From (Wu et al. 2017)

Fig. 1 Intensity-based particle size distribution (**a**), zeta potential (**b**), and AFM images (**c** and **d**) of HoA and HiN (30 mg L^{-1}). For the measurement of particle size distribution and AFM images of HoA and HiN, initial solution pH was adjusted to 5.0 by 1.0 M HCl and NaOH
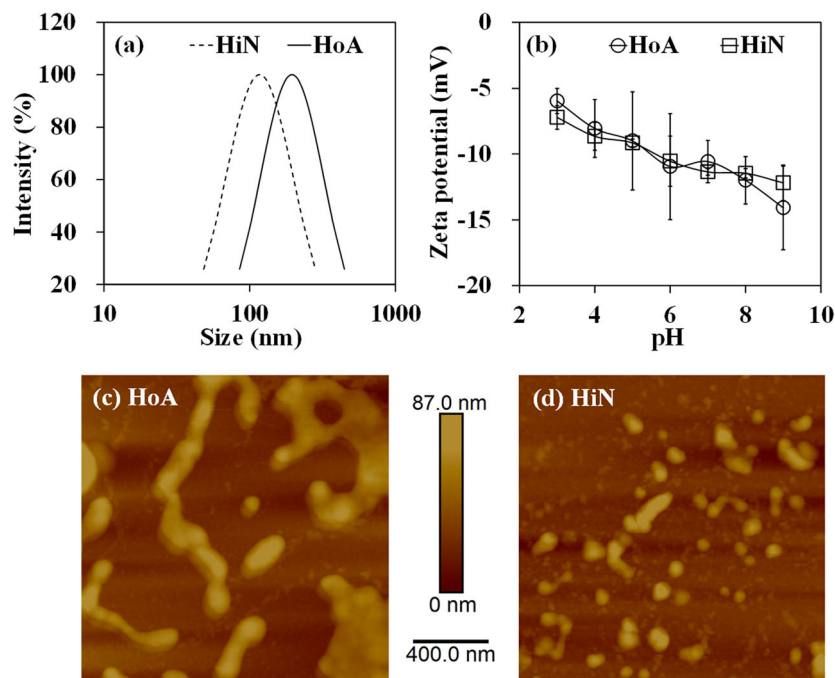
The AFM image of HoA also showed larger particles compared with that of HiN (Fig. 1c, d), which was consistent with DLS measurements. In addition, zeta potentials of HoA and HiN decreased with increasing pH (Fig. 1b), and ranged from − 5.96 to − 14.10 mV and − 7.21 to − 12.20 mV, respectively. The negative zeta potential values demonstrated that HoA and HiN were negatively charged under the experimental conditions.

From WS300 to WS700, the C content slightly increased while the H and O contents slightly decreased (Table 3). The elemental changes resulted from the higher carbonization degree of biochar at higher pyrolysis temperature, which was consistent with the loss of O-containing surface functional groups and dehydration and decarboxylation reactions (Baldock and Smernik 2002; Wu et al. 2017). Moreover, WS300 prepared at lower temperature was not fully carbonized. It could contain both noncarbonized and carbonized phase allowing partition and adsorption process (Chen et al. 2012a). When the pyrolysis temperature increased to 700 °C, the noncarbonized phase of biochar almost disappeared (Chen et al. 2012b). WS700 was mainly composed of carbonized phase. In addition, owing to the destruction of volatile organic components (e.g., aliphatic alkyl and ester groups shielding the aromatic structure) (Chen and Chen 2009; Keiluweit et al. 2010), WS700 had much higher SSA and V_{pore} than WS300 (Table 3 and Fig. 2a, d), and thus could provide more sorption sites. These physicochemical properties suggested that WS700 was more hydrophobic and aromatic compared with WS300 in which more functional groups and amorphous structures were preserved. The SSA and V_{pore} of biochars

decreased after loading of HoA and HiN (Table 3 and Fig. 2), suggesting that HoA and HiN caused surface coverage and pore blockage of biochars. Since HoA had relatively larger molecular size than HiN, it would exert more pore blockage of biochars, and thus resulted in a higher decrease of V_{pore} (Table 3).

Interactions of DOM fractions with biochars and KTP

More HoA and HiN were sorbed to biochars with increasing concentrations of them (Fig. 3). WS700 with higher SSA and V_{pore} clearly had higher sorption capacity for HoA and HiN than WS300. The max sorption capacity of WS700 was 32.17 and 18.83 times higher than that of WS300 for HoA and HiN, respectively. When KTP was added to the DOM solution for simultaneous sorption, sorption capacity of HoA and HiN to biochars decreased by 14.0–58.3% and 12.0–62.9%, respectively (Fig. 3). The results indicated that DOM fractions and KTP could compete for the same sorption sites of biochars. Since KTP was reported to interact strongly with the carbonized phase (i.e., condensed polyaromatic structures) of biochars (Wu et al. 2017), the carbonized phase could also be the main sorption domain for DOM fractions.

It can also be seen that binding affinity of HoA to WS700 was significantly higher than that of HiN (Fig. 3). The sorption capacity of WS700 for HoA was 2.23–3.32 times higher than that for HiN. The characterization results demonstrated that HoA had higher degree of aromaticity than HiN. Thus, there would be stronger specific interactions (such as π-π interactions) (Lerman et al. 2013) between HoA and carbonized phase of biochars. This was also supported by the larger
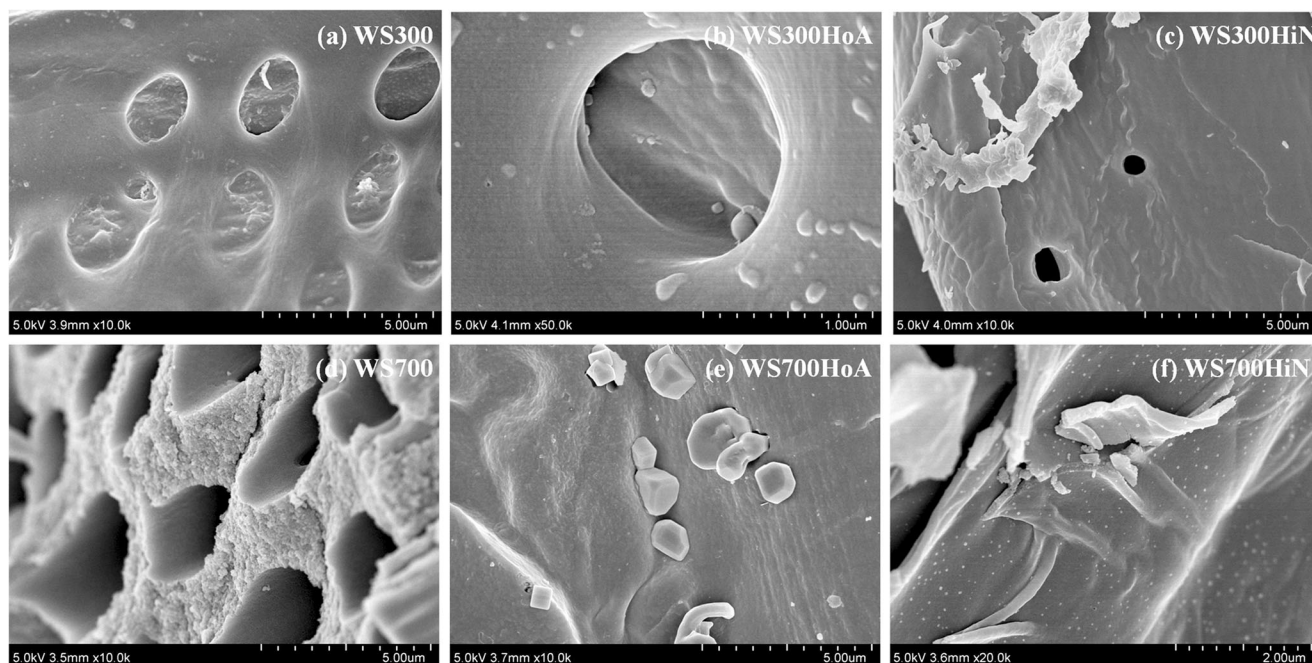
Fig. 2 SEM images of WS300 (**a**), WS300 with loaded HoA (**b**) and HiN (**c**), WS700 (**d**), and WS700 with loaded HoA (**e**) and HiN (**f**). Magnification and acceleration voltage of the SEM are shown at the bottom of the panels
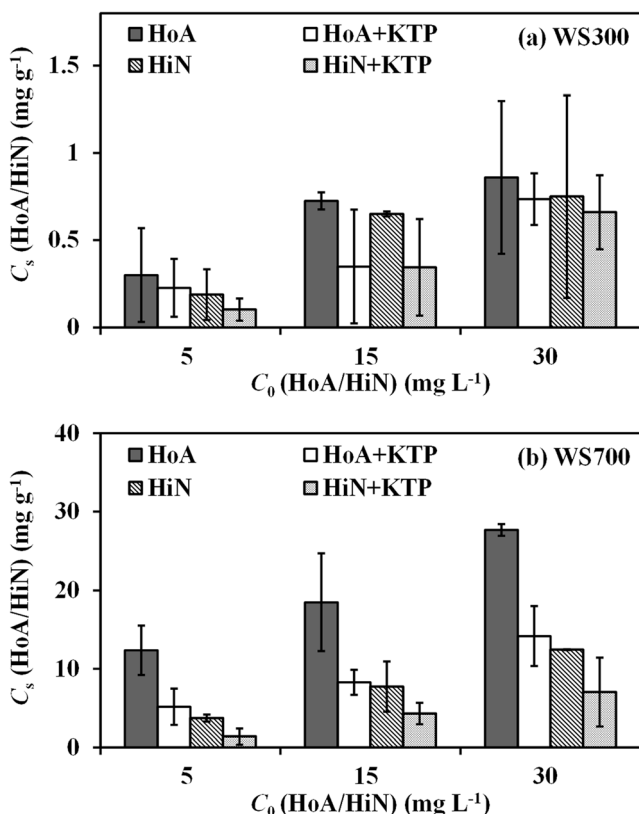

Fig. 3 Sorption of HoA and HiN to biochars with and without addition of 30 mg L^{-1} KTP in solution. C_0 is the initial concentration of HoA or HiN. Initial solution pH was adjusted to 5.0 by 1.0 M HCl and NaOH. The background electrolyte was 0.01 M NaCl

HoA and HiN sorption differences on WS700 than that on WS300 (Fig. 3), which could be due to the higher proportion of carbonized phase of WS700. In a previous study, DOM adsorptive fractionation by clay soil was elucidated (Avneri-Katz et al. 2016). The results showed that the HoA was preferentially sorbed by soil among the hydrophobic and hydrophilic fractions of DOM with up to 70% of total adsorbed carbon, which was in accord with observations of higher HoA sorption by biochars in this study.

Results of dialysis bag sorption experiments showed that KTP binding to HoA and HiN in solution at pH 3.0–9.0 was negligible with the sorption amounts measured generally equal to zero (data not shown). Meanwhile, the solubility test results (Fig. 4) showed that S_w of KTP was slightly enhanced (3%) in the presence of HoA, whereas S_w of KTP decreased (22%) in the presence of HiN. The partition coefficient of solute from the aqueous phase to DOM-containing solution can also be reflected by the solubility enhancement in the presence of DOM, assuming a partition-like interaction (Chiou et al. 1986). The small increase or even decrease in S_w of KTP indicated that association of KTP with DOM fractions in solution was very weak. This was in accordance with the results of dialysis bag sorption experiments. The reasons can be explained as follows.

HoA and HiN were negatively charged to some extent (Fig. 1b). At the same time, a previous study determined that KTP molecules (78%) existed as anionic species at pH 5.0 since the H$^+$ dissociated from -COOH group (Wu et al. 2017). Thus, the weak binding between DOM fractions and KTP could result from the electrostatic repulsion between negatively charged
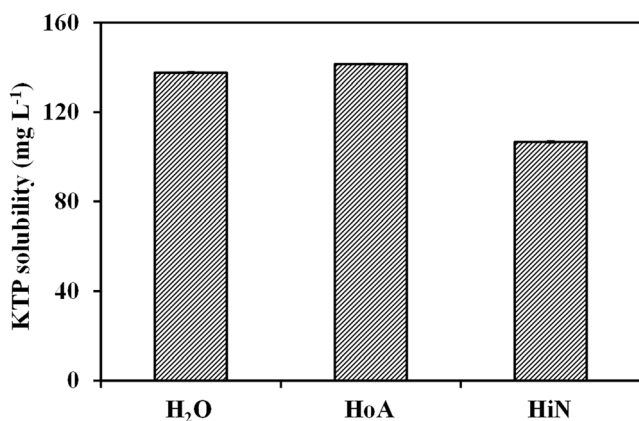
Fig. 4 Solubility of KTP in different solutions at 25 ± 1 °C. Solution pH was 5.0. Concentration of HoA and HiN was 30 mg L^{-1}. The background electrolyte was 0.01 M NaCl. The error bars representing standard errors are very short and cannot be seen

DOM fractions and anionic species of KTP. In addition, competition from water molecules gathered around HiN (Pignatello 2012) may make it difficult for KTP to interact with HiN. This also decreased the number of free water molecules available to hydrate KTP, and consequently led to obvious reduction in S_w of KTP. Since HoA, by definition, was more hydrophobic than HiN, it could have a relatively higher binding affinity with KTP, and therefore slightly enhanced S_w of KTP. Overall, however, the binding interactions between DOM fractions and KTP were very weak. Previous research also showed that binding of some pharmaceuticals (ibuprofen, carbamazepine, and sulfapyridine) to DOM in solution was insignificant (Haham et al. 2012; Hernandez-Ruiz et al. 2012), which was consistent with this study.

Effects of DOM fractions on KTP sorption to biochars

For the control samples without addition of HoA or HiN, sorption of KTP to WS700 was significantly higher than that to WS300 due to more available sorption sites of WS700 (Fig. 5 and calculated K_d values in Table 4). Since KTP sorption isotherms to both WS300 and WS700 were highly nonlinear with n values varying from 0.07–0.16 (Table 4), partition of neutral species (22% at pH 5.0) of KTP to noncarbonized phase could be insignificant, and KTP sorption to biochars was dominated by adsorption. In addition, sorption affinity of neutral species to biochars was higher than that of anionic species due to the higher hydrophobicity of the former as identified in the previous study (Wu et al. 2017).

The released DOC amount was < 3.15% of total biochar C. Assuming that the sorption coefficient of KTP to the released DOC (K_{DOC}) was as high as that to the original biochars (K_{oc}), KTP sorption to the released DOC only accounted for less than 3.15% of the total organic carbon in biochars. Furthermore, a previous study showed that the K_{oc} values of naphthalene to biochars at C_e of 0.4 solubility
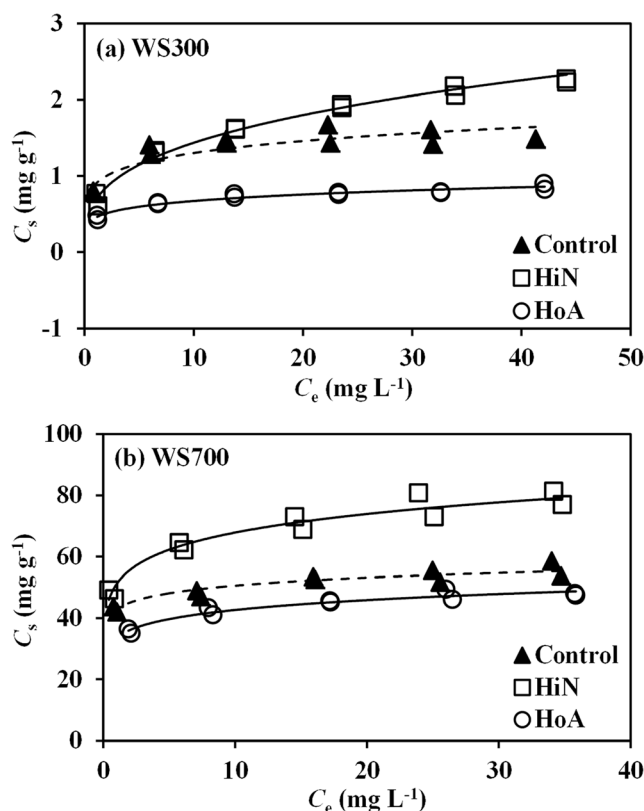

Fig. 5 Effects of HoA and HiN on KTP sorption isotherms to biochars. Each of the duplicate treatments is plotted. The black lines are the Freundlich model fitting results. Initial solution pH was adjusted to 5.0 by 1.0 M HCl and NaOH. Initial concentration of HoA and HiN was 30 mg L^{-1}. The background electrolyte was 0.01 M NaCl

(Zhang et al. 2015) were 1.3–10.2 times of the K_{DOC} value of naphthalene between dissolved humic acid and water (Pignatello et al. 2006). Therefore, it is reasonable to deduce that effect of KTP sorption to the released DOC from biochars was negligible.

Results of HoA and HiN effects on KTP sorption showed that addition of HiN in solution enhanced KTP sorption to WS300 and WS700, according to the Freundlich model (Fig. 5). The calculated K_d values of KTP to WS300 and WS700 at C_e of 20 mg L^{-1} increased by 23% and 39%, respectively, after addition of HiN (Table 4). However, sorption of KTP to biochars was inhibited when HoA was added to solution (Fig. 5). Compared to controls, the calculated K_d values at C_e of 10 and 20 mg L^{-1} decreased by 15.6–48.5% and 13.7–48.2%, respectively, after addition of HoA (Table 4). Correspondingly, the calculated Q_m values in Langmuir and Dubinin-Astakhov models also showed consistent trends (Table 4). The observed different effects of HiN and HoA on sorption of KTP to biochars indicated that they could play diverse roles. The possible reasons are discussed below.

When HoA or HiN was added to the solution system, their loading to biochars reduced the SSA and V_{pore} of biochars (Table 3). In addition, competitive sorption of KTP and

Table 4 Fitting results of isotherm models for KTP sorption to biochars in solution with and without addition of HoA or HiN (30 mg·L^{-1}) at pH 5.0

Sample	Biochar	Freundlich model					
		K_F (mg$^{(1-n)}$ L^n g^{-1})	n	R^2	RMSE[a]	K_d (L kg^{-1}) at C_e (mg L^{-1})	
						10	20
Control	WS300	0.89	0.16	0.85	0.13	130.26	72.98
Control	WS700	42.82	0.07	0.88	1.82	5055.92	2657.69
HoA	WS300	0.45	0.17	0.95	0.03	67.14	37.82
HoA	WS700	33.55	0.10	0.94	1.19	4265.80	2292.81
HiN	WS300	0.68	0.32	0.97	0.07	143.71	90.01
HiN	WS700	51.05	0.12	0.94	2.92	6785.78	3696.39
Sample	Biochar	Langmuir model					
		Q_m (mg g^{-1})	K_L (L mg^{-1})	R^2			RMSE[a]
Control	WS700	53.19	4.70	0.71			2.85
HoA	WS700	47.62	1.47	0.91			1.53
HiN	WS700	72.46	3.83	0.72			6.22
Sample	Biochar	Dubinin-Astakhov model					
		Q_m (mg g^{-1})	E (kJ mol^{-1})	b	R^2		RMSE[a]
Control	WS700	94.00	337.09	0.33	0.86		1.72
HoA	WS700	51.08	33.85	1.60	0.93		1.10
HiN	WS700	100.88	57.47	0.76	0.92		2.91

[a] RMSE $= \sqrt{\frac{1}{n}\sum_{i=1}^{n}(\text{fitted}-\text{measured})^2}$, n is the number of data points

DOM fractions on biochars occurred (Fig. 3). These factors reduced the accessibility of sorption sites for KTP, thus resulted in the inhibitory role of HoA in KTP sorption to biochars (Fig. 6). Since HoA had higher binding affinity to biochars for occupying sorption sites than HiN, it would therefore exert stronger inhibitory effects on KTP sorption to biochars. This was further demonstrated by the reduction in both K_L and E fitting parameters (Table 4), indicating the decreased sorption affinity due to the binding of DOM fractions to biochars. Similarly, the study of Zhang et al. (2015) reported humic acid coating on biochars resulted in pore blockage and surface coverage of biochars, thus weakening the sorption of

naphthalene to biochars. Moreover, inhibition of KTP sorption to WS300 (48.2–48.5%, calculated form the K_d values in Table 4) by HoA was observed to be higher than that to WS700 (13.7–15.6%). This could be because WS300 had fewer sorption sites for KTP compared with WS700 due to its smaller SSA; thus, HoA binding to WS300 exerted a greater influence on KTP sorption.

The increased KTP sorption with addition of HiN in solution indicated that the competition and loading effects of DOM fractions were not the only factors affecting KTP sorption to biochars. Recent research showed that the sorbent loaded with DOM could provide new sorption sites and facilitate

Fig. 6 Schematic diagram for KTP sorption to biochars as affected by HoA and HiN. This is an illustrative representation not drawn to scale
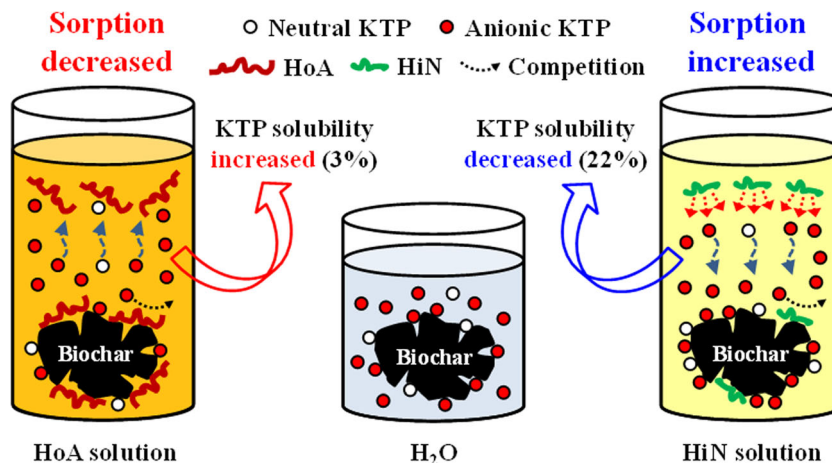
sorption of organic compounds (González-Pradas et al. 2005). However, as mentioned above, binding interactions between DOM fractions and KTP in this study were very weak due to their specific physicochemical properties. Thus, the loaded DOM fractions on biochar surfaces were not likely to serve as new sorption sites for KTP.

Solubility is a governing factor in pollutant removal by sorption (Peng et al. 2012). After excluding the factor of DOM fractions as new sorption sites for KTP, it was inferred that the increase in KTP sorption with addition of HiN could be due to the reduction in S_w of KTP in HiN solution (Fig. 4). As mentioned before, HiN would not like to bind with KTP, thereby forcing its approach to the solid biochars. Contrary to HoA (slightly improved S_w of KTP), the enhancement effects of HiN on KTP sorption by reducing S_w of KTP could exert a more dominant influence than its competitive and loading effects, thus leading to its apparent positive role in KTP sorption to biochars (Fig. 6). A previous study (Engel and Chefetz 2016) also showed the substantial influence of DOM on S_w of pollutant and its sorption. However, in that study, DOM significantly enhanced S_w of lamotrigine (by up to ~ 70%), and this led to its decreased sorption to carbon nanotubes. Moreover, the KTP sorption enhancement by HiN was more obvious on WS700 (34.2–39.1%, calculated form the K_d values in Table 4) than that on WS300 (10.3–23.3%). This could be due to the greater number of sorption sites on WS700 with higher SSA. Therefore, since addition of HiN reduced the S_w of KTP, more KTP can be sorbed to WS700 resulting in a higher degree of sorption enhancement. The impact of HiN on S_w of KTP indicates that HiN may have major effects on the mobility of such pollutant in the aquatic environment. Therefore, more attention should be paid to such changes in solubility when evaluating sorption of organic pollutants in environmental systems.

Conclusions

Loading of HoA and HiN reduced the SSA and V_{pore} of biochars. HoA also caused stronger competition with KTP on biochars than HiN due to its higher binding affinity. These factors resulted in the inhibitory role of HoA in KTP sorption to biochars by reducing the accessibility of sorption sites. The inhibition of KTP sorption by HoA was significant for biochar with lower SSA. S_w of KTP was slightly enhanced (3%) in the presence of HoA, whereas S_w of KTP decreased (22%) in the presence of HiN. The role of HiN by reducing S_w of KTP could exert a more dominant influence than its competitive and loading effects, thus enhanced KTP sorption, especially to biochar of higher SSA. The findings from this study indicated that HoA and HiN could exert varied roles in sorption of KTP, as well as other pharmaceuticals or compounds with similar structure, to biochars, which deserves more attention.

References

Avneri-Katz S, Young RB, Mckenna AM, Chen H, Corilo YE, Polubesova T, Borch T, Chefetz B (2016) Adsorptive fractionation of dissolved organic matter (DOM) by mineral soil: macroscale approach and molecular insight. Org Geochem 103:113–124

Baldock JA, Smernik RJ (2002) Chemical composition and bioavailability of thermally altered Pinus resinosa (Red pine) wood. Org Geochem 33:1093–1109

Bedard M, Giffear KA, Ponton L, Sienerth KD, Del GMV (2014) Characterization of binding between 17β-estradiol and estriol with humic acid via NMR and biochemical analysis. Biophys Chem 189:1–7

Chefetz B, Hader Y, Chen Y (1998) Dissolved organic carbon fractions formed during composting of municipal solid waste: properties and significance. Acta Hydrochim Hydrobiol 26:172–179

Chen B, Chen Z (2009) Sorption of naphthalene and 1-naphthol by biochars of orange peels with different pyrolytic temperatures. Chemosphere 76:127–133

Chen B, Zhou D, Zhu L (2008) Transitional adsorption and partition of nonpolar and polar aromatic contaminants by biochars of pine needles with different pyrolytic temperatures. Environ Sci Technol 42:5137–5143

Chen G, Lin C, Chen L, Yang H (2011) Effect of polar-dissolved organic matter fractions on the mobility of prometryne in soil. J Soils Sediments 11:395–405

Chen Z, Chen B, Chiou CT (2012a) Fast and slow rates of naphthalene sorption to biochars produced at different temperatures. Environ Sci Technol 46:11104–11111

Chen Z, Chen B, Zhou D, Chen W (2012b) Bisolute sorption and thermodynamic behavior of organic pollutants to biomass-derived biochars at two pyrolytic temperatures. Environ Sci Technol 46:12476–12483

Chiou CT, Malcolm RL, Brinton TI, Kile DE (1986) Water solubility enhancement of some organic pollutants and pesticides by dissolved humic and fulvic acids. Environ Sci Technol 20:502–508

Christensen JB, Jensen DL, Grøn C, Filip Z, Christensen TH (1998) Characterization of the dissolved organic carbon in landfill leachate-polluted groundwater. Water Res 32:125–135

Doucette WJ (2003) Quantitative structure-activity relationships for predicting soil-sediment sorption coefficients for organic chemicals. Environ Toxicol Chem 22:1771–1788

Engel M, Chefetz B (2015) Adsorptive fractionation of dissolved organic matter (DOM) by carbon nanotubes. Environ Pollut 197:287–294

Engel M, Chefetz B (2016) Removal of triazine-based pollutants from water by carbon nanotubes: impact of dissolved organic matter (DOM) and solution chemistry. Water Res 106:146–154

Fick J, Soderstrom H, Lindberg RH, Phan C, Tysklind M, Larsson DGJ (2009) Contamination of surface, ground, and drinking water from pharmaceutical production. Environ Toxicol Chem 28:2522–2527

González-Pradas E, Fernández-Pérez M, Flores-Céspedes F, Villafranca-Sánchez M, Ureña-Amate MD, Socías-Viciana M, Garrido-Herrera F (2005) Effects of dissolved organic carbon on sorption of 3,4-dichloroaniline and 4-bromoaniline in a calcareous soil. Chemosphere 59:721–728

Haham H, Oren A, Chefetz B (2012) Insight into the role of dissolved organic matter in sorption of sulfapyridine by semiarid soils. Environ Sci Technol 46:11870–11877

Hernandez-Ruiz S, Abrell L, Wickramasekara S, Chefetz B, Chorover J (2012) Quantifying PPCP interaction with dissolved organic matter in aqueous solution: combined use of fluorescence quenching and tandem mass spectrometry. Water Res 46:943–954

Ilani T, Schulz E, Chefetz B (2005) Interactions of organic compounds with wastewater dissolved organic matter: role of hydrophobic fractions. J Environ Qual 34:552–562

Jin J, Kang M, Sun K, Pan Z, Wu F, Xing B (2016) Properties of biochar-amended soils and their sorption of imidacloprid, isoproturon, and atrazine. Sci Total Environ 550:504–513

József D, Margit V, Gyula Z (2012) Biofilm controlled sorption of selected acidic drugs on river sediments characterized by different organic carbon content. Chemosphere 87:105–110

Kah M, Sigmund G, Feng X, Hofmann T (2017) Sorption of ionizable and ionic organic compounds to biochar, activated carbon and other carbonaceous materials. Water Res 124:673–692

Keiluweit M, Kleber M (2009) Molecular-level interactions in soils and sediments: the role of aromatic π-systems. Environ Sci Technol 43:3421–3429

Keiluweit M, Nico PS, Johnson MG, Kleber M (2010) Dynamic molecular structure of plant biomass-derived black carbon (biochar). Environ Sci Technol 44:1247–1253

Kumari KGID, Moldrup P, Paradelo M, Jonge LWD (2014) Phenanthrene sorption on biochar-amended soils: application rate, aging, and physicochemical properties of soil. Water Air Soil Pollut 225:2105

Leenheer JA (1981) Comprehensive approach to preparative isolation and fractionation of dissolved organic carbon from natural waters and wastewaters. Environ Sci Technol 15:578–587

Lerman I, Chen Y, Xing B, Chefetz B (2013) Adsorption of carbamazepine by carbon nanotubes: effects of DOM introduction and competition with phenanthrene and bisphenol A. Environ Pollut 182:169–176

Maoz A, Chefetz B (2010) Sorption of the pharmaceuticals carbamazepine and naproxen to dissolved organic matter: role of structural fractions. Water Res 44:981–989

Mei Y, Bai Y, Wang L (2016) Effect of pH on binding of pyrene to hydrophobic fractions of dissolved organic matter (DOM) isolated from lake water. Acta Geochim 35:1–6

Metzelder F, Funck M, Schmidt TC (2018) Sorption of heterocyclic organic compounds to multi-walled carbon nanotubes. Environ Sci Technol 52:628–637

Oh S, Shin WS, Hong TK (2016) Effects of pH, dissolved organic matter, and salinity on ibuprofen sorption on sediment. Environ Sci Pollut Res 23:22882–22889

Pan B, Zhang D, Li H, Wu M, Wang Z, Xing B (2013) Increased adsorption of sulfamethoxazole on suspended carbon nanotubes by dissolved humic acid. Environ Sci Technol 47:7722–7728

Peng H, Pan B, Wu M, Liu R, Zhang D, Wu D, Xing B (2012) Adsorption of ofloxacin on carbon nanotubes: solubility, pH and cosolvent effects. J Hazard Mater 211-212:342–348

Peuravuori J, Pihlaja K (1997) Molecular size distribution and spectroscopic properties of aquatic humic substances. Anal Chim Acta 337:133–149

Pignatello JJ (2012) Dynamic interactions of natural organic matter and organic compounds. J Soils Sediments 12:1241–1256

Pignatello JJ, Kwon S, Lu Y (2006) Effect of natural organic substances on the surface and adsorptive properties of environmental black carbon (char): attenuation of surface activity by humic and fulvic acids. Environ Sci Technol 40:7757–7763

Polubesova T, Sherman-Nakache M, Chefetz B (2007) Binding of pyrene to hydrophobic fractions of dissolved organic matter: effect of polyvalent metal complexation. Environ Sci Technol 41:5389–5394

Shimabuku KK, Cho H, Townsend EB, Rosario-Ortiz FL, Summers RS (2014) Modeling nonequilibrium adsorption of MIB and sulfamethoxazole by powdered activated carbon and the role of dissolved organic matter competition. Environ Sci Technol 48:13735–13742

Straathof AL, Comans RN (2015) Input materials and processing conditions control compost dissolved organic carbon quality. Bioresour Technol 179:619–623

Stuart M, Lapworth D, Crane E, Hart A (2012) Review of risk from potential emerging contaminants in UK groundwater. Sci Total Environ 416:1–21

Tixier C, Singer HP, Oellers S, Muller SR (2003) Occurrence and fate of carbamazepine, clofibric acid, diclofenac, ibuprofen, ketoprofen, and naproxen in surface waters. Environ Sci Technol 37:1061–1068

Wu L, Li B, Bi E (2017) Effect of molecular dissociation and sorbent carbonization on bisolute sorption of pharmaceuticals by biochars. Water Air Soil Pollut 228:242

Xiao L, Bi E, Du B, Zhao X, Xing C (2014) Surface characterization of maize-straw-derived biochars and their sorption performance for MTBE and benzene. Environ Earth Sci 71:5195–5205

Xu J, Chen W, Wu L, Chang AC (2009) Adsorption and degradation of ketoprofen in soils. J Environ Qual 38:1177–1182

Xue S, Zhao QL, Wei LL, Ren NQ (2009) Behavior and characteristics of dissolved organic matter during column studies of soil aquifer treatment. Water Res 43:499–507

Yang NW, Bi EP (2017) Effects of dissolved organic matter fractions extracted from humus soil on sorption of benzotriazole in brown soil and back soil. Environ Sci 38:2568–2576 **(in Chinese)**

Yang L, He JT, Su SH, Cui YF, Huang DL, Wang GC (2017) Occurrence, distribution, and attenuation of pharmaceuticals and personal care products in the riverside groundwater of the Beiyun River of Beijing, China. Environ Sci Pollut Res 24:15838–15851

Zhang M, Shu L, Guo X, Shen X, Zhang H, Shen G, Wang B, Yang Y, Tao S, Wang X (2015) Impact of humic acid coating on sorption of naphthalene by biochars. Carbon 94:946–954

Zhang F, Li Y, Zhang G, Li W, Yang L (2017) The importance of nano-porosity in the stalk-derived biochar to the sorption of 17β-estradiol and retention of it in the greenhouse soil. Environ Sci Pollut Res 24:9575–9584